Reducing environmental footprint from a new air gun design

Mehul Supawala*, David Gerez and Halvor Groenaas, WesternGeco; Jon-Fredrik Hopperstad and Robert Laws, Schlumberger Gould Research

This paper was prepared for presentation during the 15th International Congress of the Brazilian Geophysical Society held in Rio de Janeiro, Brazil, 31 July to 3 August, 2017.

Abstract

We developed a new air gun that optimizes the useful seismic output while limiting environmental effects from unnecessary high-frequency emissions.The environmental benefit of such a source is demonstrated and we show that the resulting seismic image acquired with the new source is identical to the one acquired with standard sources. Ceteceans, including species offshore Brazil, will benefit from the reduced emissions. Figure 1 shows an example of the new air-gun design.

We also compare the 'risk of hearing damage' to marine mammals calculated from experimental measurements made with two different types of sources, one type is a standard air gun that is used ubiquitously; the other is a new design with attenuated high-frequency output, a lower peak pressure and a smoother pulse onset (Coste et al., 2014). The newly designed air gun has been in use on a commercial seismic survey since December 2016.

Figure 1 *- An example of the new design of air gun.*

Introduction

Marine seismic operations are the subject of increasing environmental scrutiny.

Several earlier studies of the spatial zone over which injury might be caused to marine mammals by seismic sources were based on the Southall *et al.* (2007) criteria (Breitzke and Bohlen, 2010; Laws, 2010; Laws, 2013; Goertz *et al.*, 2013). NOAA (2013) and Southall (2007) provide metrics for the risk of hearing damage. These metrics are the received peak pressure, which is the maximum acoustic pressure experienced by the animal, and the sound exposure level (SEL), which is the integral over 24 hours of the spectrally weighted (the M weighting) received acoustic energy. The marine mammals are categorised by their hearing into five groups and there is a different M weighting and hearing damage for each group. NOAA has revised the M weighting curves and the hearing damage thresholds from those originally given by Southall *et al.* (2007) following more recent bioacoustics research. We used the NOAA (2013) guidelines in this abstract.

In Figure 2, we plot the total energy in all directions from a 4410-in^3 standard source, emitting energy every 10 s. We also plot the cetecean sensitivity through the M weighting from the NOAA (2013) guideline. The product of the total source energy and cetecean sensitivity gives the weighted power spectrum shown in Figure 3. The area under this curve is proportional to the SEL. We consider that the useful frequency for imaging rapidly declines beyond 100 Hz. It is, therefore, apparent that our sources release much more energy into the environment than is required for seismic imaging.

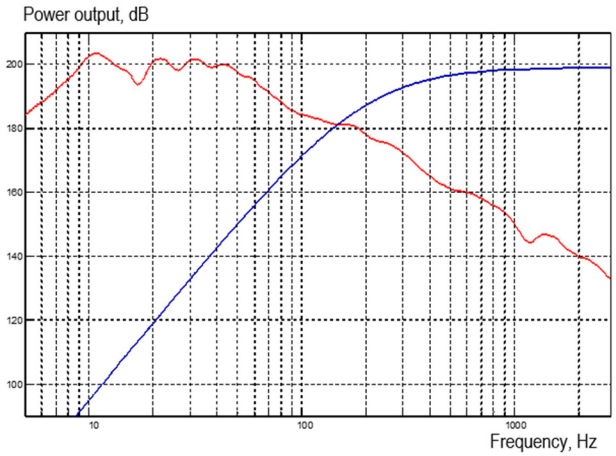

Figure 2 *- The total acoustic energy in all directions from a 4410-in^3 source firing every 10 s is shown in red. The high-frequency cetecean sensitivity from NOAA (2013) guideline is shown in blue.*

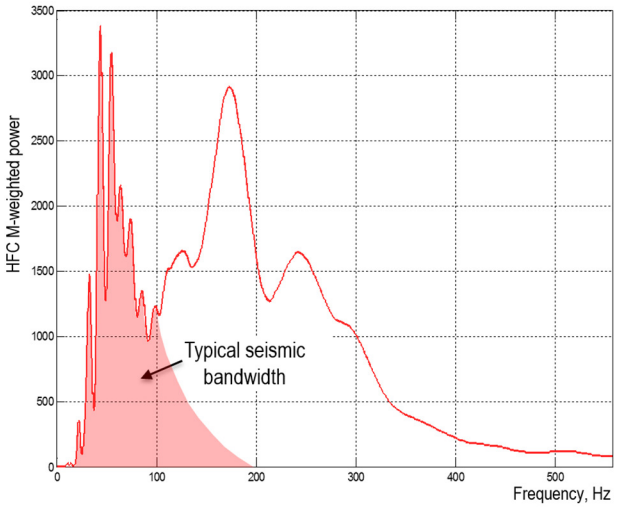

Figure 3 *- The weighted power spectrum of a 4410-in^3 source with standard air guns. The shaded area represents the typical seismic bandwidth.*

Design method

The high-frequency output of air guns comes primarily from the rising edge of the start for the seismic pulse, when the air is initially released from the air gun (Coste *et al*., 2014). Herein, we use an example of a standard 290-in^3 air gun as illustrated in Figure 4, which shows an example near-field air-gun pulse of a standard 290-in^3 air gun. On the first panel, we plot the cummulative energy over the entire acoustic pulse over 3 Hz to 25-kHz bandwidth. In the second panel we apply a high-cut filter at 80 Hz plotting only the energy from 3 to 80 Hz, which we consider the typical frequency range for seismic imaging at the reservior level. The shape of the wavelet is quite similar to the full bandwidth version, especially the bubble train. In the third panel; we apply an equivalent low-cut filter at 80 Hz. It is clear that most of the cumulative energy (above 80 Hz) is emitted during the onset of the pulse.

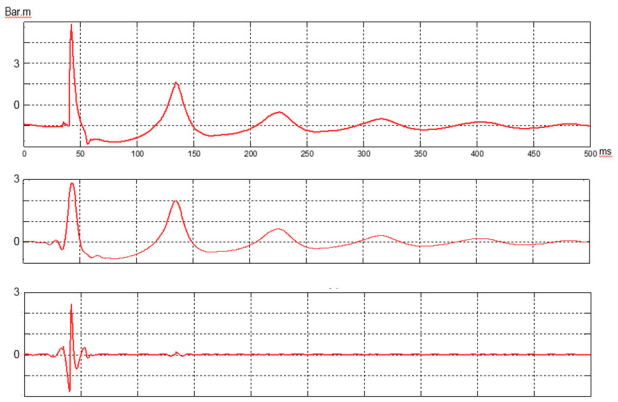

Figure 4 *- A near-field measurement for standard 290-in^3 air-gun pulse. Top panel shows the total cumulative energy over the entire acoustic pulse from the 3 Hz to 25-kHz bandwidth. The second panel with a high-cut filter at 80 Hz confirms the shape of wavelet similar to the full bandwidth version, especially the bubble train. The third panel with a low-cut filter at 80 Hz clearly shows that the bulk of the emitted energy above 80 Hz comes from the rising edge of the pulse.*

The new air-gun design regulates the release of air at a much slower rate compared to standard air guns. It does this through a port that opens gradually and precise control of the piston speed inside the new air gun.

The new air-gun design is inherently modular and can be configured in the field with three different corner frequencies and filter roll-offs by replacing a single mechanical component as shown in Figure 5.

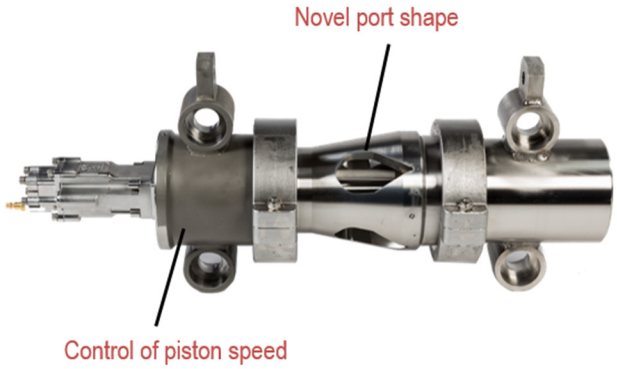

Figure 5 *- New air-gun design. Note the novel port shape and compotent controlling the speed of air-gun piston, enabling multiple configurations.*

Acoustic output comparison

The acoustic output from the new air-gun design is characterized for different air volumes and depths as well as cluster and non-cluster configurations. Figure 6 shows the comparison for the amplitude spectra for a 150-in^3 air gun for a standard design and the new design with the three different configurations.

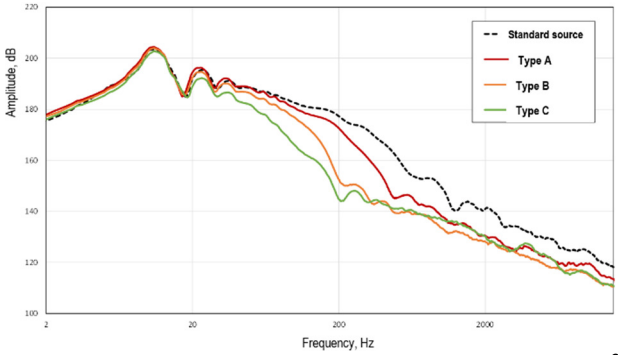

Figure 6 *- Comparison of amplitude spectra for a 150-in^3 air gun for a standard design and the new design.*

We re-compute the weighted power spectrum from Figure 2, but with measurements from the new air-gun design. As illustrated in Figure 7, it is clear that the unwanted portion of the weighted power spectrum reduces significantly with the new Type-A air-gun design and is further reduced with Types B and C.

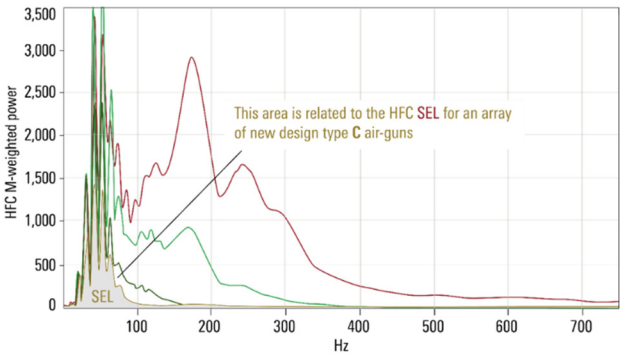

Figure 7 *- Comparison of the weighted power spectrum of a 4410-in^3 source with standard air-gun design with the new design. The area under the curves is propotional to the SEL for high-frequency cetecean sensitivity based on NOAA 2013 criteria).*

The NOAA (2013) risk of hearing damage around seismic source

Using the NOAA (2013) guidelines, we calculate the risk of hearing damage zones for ceteceans sensitive to high frequencies. The injury zone is the area around the source within which the cetecean has the potential to get injured. There are several ways to model this, which also depends on the type of cetacean class. In this study we look at high-frequency cetaceans, and assume the source and animal remain static relative to each other for 1 hour, with the same 4410-in^3 source firing every 10 s. A simple ocean propagation model is used.

Figure 8 shows a frame encompassing a distance of 1 km in each direction away from the source location as indicated by the small blue dot at the sea surface. The red surface represents the injury zone for a high-frequency mammal based on the SEL criteria and the green surface represents the injury zone based on peak pressure criteria from the NOAA (2013) guideline. It is very clear that the new design has dramatically reduced the overall zone within which there is risk of hearing damage.

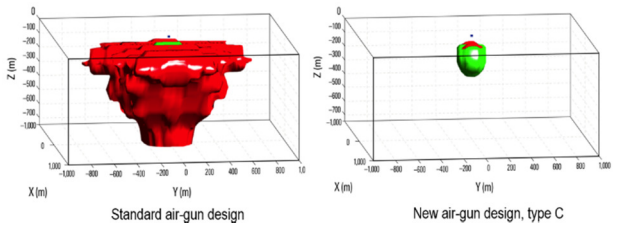

Figure 8 *- Comparison of risk of hearing damage zones for standard air-gun design and the new air-gun design.*

Comparison of seismic images

We conducted a field test with a standard air-gun source and the new Type-A air-gun source in a flip-flop acquisition mode. Recording was done on the same streamer system over the same geology.

Figure 9 shows two seismic images processed from the flip-flop line. One image is from the flip source (standard air guns) and the other image is from the flop source (the new air-gun design in its Type-A configuration). The images are essentially identical; there is no geophysical disadvantage to using the new air-gun design.

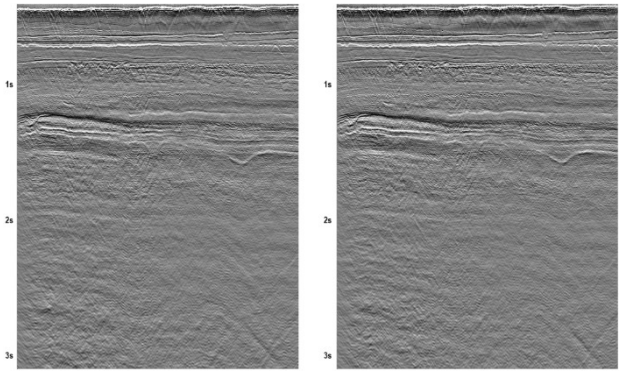

Figure 9 *- Post-migrated stacks for the new air-gun designarray Type A (left panel) and the standard air-gun array (right). The images obtained are practically identical.*

Conclusions

A new air-gun design was developed to control the shape of the seismic pulse. As a result, the new design emits significantly less energy above the seismic band of interest than a standard air gun..

The environmental impacts of two different types of air guns were compared at a variety of ranges. The new type of air gun produces a significantly lower SEL per shot than does the standard type.

The 'risk of hearing damage' zone (as defined by the NOAA (2013) guidelines) around a seismic source is significantly reduced with the new design.

The seismic images produced by the two types or air guns are essentially the same and the output can be tailored to imaging needs.

Acknowledgments

In addition to the authors, many people contributed to the development of this new air-gun design. Among them are: Jostein Farstad, Martin Howlid, Edward Kotochigov, Kambiz Iranpour, Lars Roenning, Anneli Soppi, Morten Svendsen, Johan-Fredrik Synnevåg, Rune Voldsbekk, and Luren Yang.

We also thank David Halliday, Ed Kragh, Peter Watterson, Catalina Llano Ocampo and the crew of the vessel 'Amazon Conqueror' for thier valuable help with this study.

References

GEREZ, D., GROENAAS, H., PRAMM LARSEN, O., WOLFSTIRN, M., PADULA, M. 2015. Controlling air-gun output to optimize seismic content while reducing unnecessary high-frequency emission. 85th Annual

International Meeting, SEG, Expanded Abatracts, 154-158.

COSTE, E., GEREZ, D., GROENAAS, HOPPERSTAD, J.F., H., PRAMM LARSEN, O., LAWS, R.M., NORTON, J., PADULA, M. AND WOLFSTIRN, M. 2014. Attenuated high-frequency emission from a new design of air-gun. 84th Annual International Meeting, SEG, Expanded Abstracts, 132-137.

LAWS, R.M. 2013. Modifying the Seismic Source Array Spectrum to Reduce the Risk of Hearing damage to Marine Mammals. 75th EAGE Conference and Exhibition, Extended Abstracts, TH1615.

LAWS, R.M. 2010. Cetacean hearing-damage zones around a seismic source. in A.N. Popper and A. Hawkins (Eds.), The Effects of Noise on Aquatic Life, Advances in Experimental Medicine and Biology. 730, 473-476, DOI 10.1007/978-1-4419-7311-5_107, © Springer Science+Business Media, LLC 2012.

BREITZKE, M. AND BOHLEN, T. 2010. Modelling cumulative sound exposure along a seismic line to assess the risk of seismic research surveys on marine mammals in the Antarctic treaty area. in A.N. Popper and A. Hawkins (Eds.), The Effects of Noise on Aquatic Life, Advances in Experimental Medicine and Biology. 730, Springer Science+Business Media, LLC, 2012, 609-611.

GOERTZ, A., WISLØFF, J.F. DROSSAERT, F AND ALI J. 2013. Environmental source modelling to mitigate impact on marine life. First Break, 31(11), 59-64

HOPPERSTAD, J-F, SYNNEVAAG J-F. AND SOPPI, A. 2005. Method and apparatus for controlling the acoustic output of an air-gun. US patent 7321527.

LAWS, R. M. 2010. Cetacean hearing-damage zones around a seismic source, in A.N. Popper and A. Hawkins (Eds.), The Effects of Noise on Aquatic Life, Advances in Experimental Medicine and Biology. 730, Springer Science+Business Media, LLC 2012, 473-475

LUCKE, K. U., SIEBERT, U., P. LEPPER, P.A. AND BLANCHET, M.A. 2009. Temporary shift in masked hearing thresholds in a harbor porpoise (Phocoena phocoena) after exposure to seismic air-gun stimuli. Journal of the Acoustical Society of America, 125, 4060–4070

NOAA. 2013. Draft Guidance for Assessing the Effects of Anthropogenic Sound on Marine Mammals, Acoustic Threshold Levels for Onset of Permanent and Temporary Threshold Shifts Draft: 23 December 2013, http://www.nmfs.noaa.gov/pr/acoustics/guidelines.htm.

SOUTHALL, B. L., BOWLES, A.E., ELLISON, W.T. FINNERAN, J.J., GENTRY, R.L., GREENE, C.R., KASTAK, D., KETTEN, D.R., MILLER, J.F., NACHTIGALL, P.E., RICHARDSON, W.-J., THOMAS, J.A. AND TYACK, **P.L.** 2007. Marine mammal noise exposure criteria: Initial scientific recommendations. Aquatic Mammals, 33, 411–522 ISSN 0167-5427.

ZIOLKOWSKI, A. M., PARKES, G.F., HATTON, L. AND HAUGLAND, T. 1982. The signature of an air gun array: Computation from near-field measurements including interactions. Geophysics, 47(10), 1413–1421.